NUMERICAL LINEAR ALGEBRA WITH APPLICATIONS
Numer. Linear Algebra Appl. 2001; **8**:551–570 (DOI: 10.1002/nla.263)

A multilevel Newton–Krylov interface solver for multiphysics couplings of flow in porous media

Ivan Yotov*,†

Department of Mathematics, University of Pittsburgh, Pittsburgh, PA 15260, U.S.A.

SUMMARY

A multiblock approach to modelling flow in porous media allows for coupling different physical and numerical models in a single simulation through the use of mortar finite elements. The resulting non-linear algebraic system is reduced to a non-linear interface problem which is solved by a full approximation scheme (FAS) multigrid with a Newton-GMRES smoother. Copyright © 2001 John Wiley & Sons, Ltd.

KEY WORDS: multiphysics; multigrid; multiblock; mortar finite elements; non-matching grids; domain decomposition; Newton–Krylov methods; multiphase flow

1. INTRODUCTION

Energy and environmental applications of flow in porous media modelling usually involve solving systems of tens of millions of unknowns. The large scale is due to the size of the simulation domain and the multiscale nature of the physical processes. Non-linearities due to the presence of multiple flowing phases add another degree of difficulty to the problem. Very often, however, the complexity of the physics varies throughout the domain of interest. For example, in enhanced oil recovery, natural gas often forms near production wells, but may not be present away from them. A recently developed multiblock multiphysics formulation decomposes the domain into a series of blocks (subdomains) and allows different physical models, grids, and numerical methods to be used in different blocks [1–4]. Careful choice of physical models and discretization schemes may lead to substantial computational savings without sacrificing accuracy.

* Correspondence to: Ivan Yotov, Department of Mathematics, 301 Thackeray Hall, University of Pittsburgh, Pittsburgh, PA 15260, USA.
† E-mail: yotov@math.pitt.edu.

Contract/grant sponsor: DOE; contract/grant number: DE-FGO 3-99ER25371
Contract/grant sponsor: NSF; contract/grant number: DMS98733266
Contract/grant sponsor: University of Pittsburgh; contract/grant number: CRDF grant
Contract/grant sponsor: Sloan Foundation; contract/grant number: 99-5-9AP

Received 30 October 2000
Revised 2 August 2001

Mixed finite element methods are employed for subdomain discretizations due to their local mass conservation property. The subdomains are coupled through physically meaningful interface conditions in a numerically stable and accurate way. This is achieved by introducing mortar finite elements along the interfaces [1, 2] (see Section 3 for a detailed discussion).

Another critical issue is how to solve efficiently the non-linear algebraic system that arises in the multiblock multiphysics discretization of multiphase flow in porous media, which is the main subject of this paper. Because of the complexity of the formulation, loose coupling between subdomains is desired. This is accomplished by reducing the global system to a non-linear interface problem. The algorithm is based on a non-overlapping domain decomposition algorithm originally proposed by Glowinski and Wheeler [5–7] for linear single block problems and later extended to multiblock elliptic problems [1, 8] and two-phase flow problems [9]. Other substructuring algorithms for mortar finite elements can be found in References [10–12]. In its non-linear version [9] our method can be viewed as a non-overlapping counterpart of some overlapping non-linear domain decomposition methods [13, 14]. Here we formulate the algorithm for multiblock multiphysics couplings. A new feature in this case is that the number of interface variables may be different on different interfaces. Our approach is suitable for parallel implementation and allows for relatively easy coupling of existing simulators, since subdomain solves represent the dominant computational cost.

We introduce two methods for the solution of the non-linear interface problem: an inexact Newton-GMRES method [15] and a full approximation scheme (FAS) multigrid V-cycle [16] with Newton-GMRES smoothing. The idea of using an inexact Newton step as a non-linear smoother is new to the best of our knowledge. The efficiency of both methods depends on the convergence of GMRES for computing the inexact Newton step. A physics-based Neumann–Neumann preconditioner is constructed for accelerating the GMRES convergence.

The interface operator involves the solution of subdomain problems with Dirichlet boundary conditions specified by the current values of primary interface variables. Different choices of primary variables are possible, affecting the mathematical properties of the operator [4]. We shall discuss the implementation of the interface GMRES preconditioner for the various choices and its effectiveness in handling degeneracies of the interface operator.

The rest of the paper is organized as follows. In the next section we present a multiblock formulation for coupling single-phase, two-phase, and three-phase flow in porous media. The multiblock discretization is given in Section 3. In Section 4 we describe the domain decomposition solvers and preconditioners. Computational results are given in Section 5. The paper ends with conclusions in Section 6.

2. MULTIBLOCK MULTIPHYSICS MODEL

In a multiblock formulation, the domain $\Omega \subset \mathbf{R}^3$, is decomposed into a series of subdomains $\Omega_k,\ k = 1, \ldots, n_b$. Let $\Gamma_{kl} = \partial\Omega_k \cap \partial\Omega_l$ be the interface between Ω_k and Ω_l. A physical model is associated with each block. We consider three possible models — single-phase (water) flow, two-phase (water and oil) flow, and three-phase (water, oil, and gas) flow, which commonly occur in reservoir simulation. Each model is described by a set of differential equations derived from a more general compositional model [17]. In particular, there are three components,

W — water, O — oil, and G — gas, distributed among three phases, w — water, o — oil, and g — gas.

2.1. Single-phase model

This model assumes that only one phase (w — water) is present and consists of one component (W — water). The flow is governed by the conservation of mass equation for W

$$\frac{\partial(\phi N_{\mathrm{W}})}{\partial t} + \nabla \cdot \mathbf{U}_{\mathrm{W}} = q_{\mathrm{W}} \tag{1}$$

where $N_{\mathrm{W}} = \rho_{\mathrm{w}}$ is the component concentration, $\rho_{\mathrm{w}} = \rho_{\mathrm{w}}(P_{\mathrm{w}})$ is the phase density, ϕ is the porosity, q_{W} is the source term, and

$$\mathbf{U}_{\mathrm{W}} = \mathbf{U}_{\mathrm{w}} = -\frac{K}{\mu_{\mathrm{w}}}\rho_{\mathrm{w}}(\nabla P_{\mathrm{w}} - \rho_{\mathrm{w}} g \nabla D) \tag{2}$$

is the Darcy velocity of phase w. Here P_{w} is the water phase pressure, μ_{w} is the phase viscosity, K is the rock permeability tensor, g is the gravitational constant, and D is the depth. We note that this is a mildly non-linear system, since the only non-linearity is $\rho_{\mathrm{w}} = \rho_{\mathrm{w}}(P_{\mathrm{w}})$ and the fluid is assumed slightly compressible.

2.2. Two-phase model

In this case both water phase w and oil phase o are present. The water component W exists only in the water phase and the oil component O exists only in the oil phase. Let $N_{\mathrm{W}} = \rho_{\mathrm{w}} S_{\mathrm{w}}$ and $N_{\mathrm{O}} = \rho_{\mathrm{o}} S_{\mathrm{o}}$ be the component concentrations, and let $\mathbf{U}_{\mathrm{W}} = \mathbf{U}_{\mathrm{w}}$ and $\mathbf{U}_{\mathrm{O}} = \mathbf{U}_{\mathrm{o}}$ be the component fluxes. The governing equations are

$$\frac{\partial(\phi N_{\mathrm{W}})}{\partial t} + \nabla \cdot \mathbf{U}_{\mathrm{W}} = q_{\mathrm{W}} \tag{3}$$

$$\frac{\partial(\phi N_{\mathrm{O}})}{\partial t} + \nabla \cdot \mathbf{U}_{\mathrm{O}} = q_{\mathrm{O}} \tag{4}$$

$$\mathbf{U}_{\alpha} = -\frac{k_{\alpha}(S_{\alpha})K}{\mu_{\alpha}}\rho_{\alpha}(\nabla P_{\alpha} - \rho_{\alpha} g \nabla D) \tag{5}$$

where $\alpha = \mathrm{w}$, o denotes the phase, S_{α} are the phase saturations, and $k_{\alpha}(S_{\alpha})$ are the phase relative permeabilities. The above equations are coupled via the volume balance equation and the oil–water capillary pressure relation

$$S_{\mathrm{w}} + S_{\mathrm{o}} = 1, \quad p_{\mathrm{cow}}(S_{\mathrm{w}}) = P_{\mathrm{o}} - P_{\mathrm{w}}. \tag{6}$$

2.3. Black-oil model

This model allows for all three phases and components to be present. The water component W exists only in the water phase w, the oil component O exists only in the oil phase o, while the gas component G is distributed among the oil phase o and the gas phase g according to

the *gas–oil ratio* $R_s(P_o)$ [18]. The conservation equations are written for the components as they appear on the surface, at *stock-tank conditions* (STC):

$$\frac{\partial(\phi \bar{N}_W)}{\partial t} + \nabla \cdot \bar{\mathbf{U}}_W = \bar{q}_W \tag{7}$$

$$\frac{\partial(\phi \bar{N}_O)}{\partial t} + \nabla \cdot \bar{\mathbf{U}}_O = \bar{q}_O \tag{8}$$

$$\frac{\partial(\phi \bar{N}_G)}{\partial t} + \nabla \cdot \bar{\mathbf{U}}_G = \bar{q}_G \tag{9}$$

where

$$\bar{N}_W = \frac{S_w}{B_w}, \quad \bar{N}_O = \frac{S_o}{B_o}, \quad \bar{N}_G = \frac{S_g}{B_g} + R_s \frac{S_o}{B_o}$$

are the component concentrations,

$$\bar{\mathbf{U}}_W = \frac{\mathbf{U}_w}{B_w}, \quad \bar{\mathbf{U}}_O = \frac{\mathbf{U}_o}{B_o}, \quad \bar{\mathbf{U}}_G = \frac{\mathbf{U}_g}{B_g} + R_s \frac{\mathbf{U}_o}{B_o}$$

are the component fluxes,

$$B_w = \frac{\rho_W^{STC}}{\rho_w}, \quad B_g = \frac{\rho_G^{STC}}{\rho_g}, \quad B_o = \frac{\rho_O^{STC} + R_s \rho_G^{STC}}{\rho_o}$$

are the *formation volume factors*, ρ_i^{STC}, $i = W, O, G$ are the component densities at STC, $\bar{q}_i = q_i / \rho_i^{STC}$ are the component sources, and

$$\mathbf{U}_\alpha = -\frac{k_\alpha(S_\alpha)K}{\mu_\alpha} \rho_\alpha (\nabla P_\alpha - \rho_\alpha g \nabla D), \quad \alpha = w, o, g \tag{10}$$

are the phase Darcy velocities. Here we use bars to denote variables at STC. Throughout the rest of the paper we will omit the bars to simplify the notation.

The model is completed with

$$S_w + S_o + S_g = 1, \quad p_{cow}(S_w) = P_o - P_w, \quad p_{cgo}(S_g) = P_g - P_o. \tag{11}$$

The relationships $R_s(P_o)$, $B_w(P_w)$, $B_o(P_o)$, $B_g(P_g)$, $p_{cow}(S_w)$, and $p_{cgo}(S_g)$ are available from measurements [18].

2.4. Interface conditions

To complete the multiblock formulation we need to impose matching conditions on subdomain interfaces and boundary conditions on the outside boundary.

On each interface Γ_{kl} the following physically meaningful continuity conditions are imposed:

$$P_\alpha|_{\Omega_k} = P_\alpha|_{\Omega_l} \quad \text{on } \Gamma_{kl} \tag{12}$$

$$[\mathbf{U}_i \cdot v]_{kl} \equiv \mathbf{U}_i|_{\Omega_k} \cdot v_k + \mathbf{U}_i|_{\Omega_l} \cdot v_l = 0 \quad \text{on } \Gamma_{kl} \tag{13}$$

where v_k denotes the outward unit normal vector on $\partial\Omega_k$. Equations (12) and (13) represent continuity of pressures and normal fluxes, respectively (the plus sign in (13) is due to the

opposite orientation of the normals on the two subdomains). The sets of phase indexes α and component indexes i for which the above conditions are imposed depend on the physical models imposed on the neighboring blocks. In particular, let Γ^1 be the union of all interfaces for which at least one of the neighbouring subdomain models is single phase, let Γ^2 be the union of all 'two-phase/two-phase' and 'two-phase/black-oil' interfaces, and let Γ^3 be the union of all black-oil/black-oil interfaces. Equations (12) and (13) then hold for $\alpha = \mathrm{w}$ and $i = \mathrm{W}$ on Γ^1, for $\alpha = \mathrm{w}, \mathrm{o}$ and $i = \mathrm{W}, \mathrm{O}$ on Γ^2, and for $\alpha = \mathrm{w}, \mathrm{o}, \mathrm{g}$ and $i = \mathrm{W}, \mathrm{O}, \mathrm{G}$ on Γ^3.

In addition, the appropriate volume balance and capillary pressure relationships (6) or (11) are assumed to hold on multiphase interfaces.

We assume for simplicity that no flow $\mathbf{U}_i \cdot \nu = 0$ is imposed on $\partial\Omega$, although more general types of boundary conditions can also be treated.

Remark 2.1

We note that, in order for the multiphysics formulation to make sense, we must assume that the oil phase is not present in a two-phase domain near a single-phase interface, and that the gas phase is not present in a black-oil domain near a two-phase interface. If this is not true at any time, then the interface must be moved or removed, which can be done dynamically during the simulation. (See References [3, 4, 19] for more details about the multiphysics couplings.)

3. MULTIBLOCK DISCRETIZATION

The subdomain equations are discretized by the lowest order Raviart–Thomas mixed finite element spaces RT_0 [20]. Consider a rectangular partition of Ω_k by $\mathscr{T}_{h_k}$, where h_k is associated with the size of the elements. The RT_0 spaces are defined on $\mathscr{T}_{h_k}$ by

$$\begin{aligned}
\tilde{\mathbf{V}}_{h_k} = \{&\mathbf{v} = (v_1, v_2, v_3) : \mathbf{v}|_E = (\alpha_1 x_1 + \beta_1, \alpha_2 x_2 + \beta_2, \alpha_3 x_3 + \beta_3)^{\mathrm{T}} : \\
&\alpha_l, \beta_l \in \mathbf{R} \text{ for all } E \in \mathscr{T}_{h_k} \\
&\text{and each } v_l \text{ is continuous in the } l\text{th co-ordinate direction}\}
\end{aligned}$$

$$\mathbf{V}_{h_k} = \{\mathbf{v} \in \tilde{\mathbf{V}}_{h_k} : \mathbf{v} \cdot \nu_k = 0 \text{ on } \partial\Omega_k \cap \partial\Omega\}$$

$$W_{h_k} = \{w : w|_E = \alpha : \alpha \in \mathbf{R} \text{ for all } E \in \mathscr{T}_{h_k}\}.$$

To impose the interface matching condition (12)–(13) we introduce a Lagrange multiplier or mortar finite element space (see References [21–23] for the standard finite element and Reference [24] for finite volume element formulation). Mortar mixed finite element methods have been studied for elliptic problems in References [1, 2, 25] and for the Stokes problem in Reference [26]. Optimal convergence is also shown for the case of a degenerate parabolic equation arising in two phase flow in porous media [27]. Multiphysics applications can be found in Reference [3].

The mortar finite element space $M_{h_{kl}}$ is defined on a rectangular grid $\mathscr{T}_{h_{kl}}$ on Γ_{kl}, where h_{kl} is associated with the size of the elements in $\mathscr{T}_{h_{kl}}$. In this space we approximate the interface pressures and concentrations, and impose weakly normal continuity of fluxes.

If the subdomain grids adjacent to Γ_{kl} match, we take $\mathcal{T}_{h_{kl}}$ to be the trace of the subdomain grids and define the matching mortar space by

$$M^m_{h_{kl}} = \{\mu:\ \mu|_e = \alpha:\ \alpha \in \mathbf{R},\ \text{for all } e \in \mathcal{T}_{h_{kl}}\}.$$

If the grids adjacent to Γ_{kl} are non-matching, the interface grid need not match either of them. A mild condition on $\mathcal{T}_{h_{kl}}$ to guarantee solvability and accuracy of the numerical scheme must be imposed (see Remark 3.3). We define our non-matching mortar space on an element $e \in \mathcal{T}_{h_{kl}}$ by

$$M^n_h(e) = \{\alpha\xi_1\xi_2 + \beta\xi_1 + \gamma\xi_2 + \delta:\ \alpha, \beta, \gamma, \delta \in \mathbf{R}\}$$

where ξ_l are the co-ordinate variables on e. Then, for each Γ_{kl}, we give two possibilities for the non-matching mortar space, a discontinuous and a continuous version, as

$$M^{n,d}_{h_{kl}} = \{\mu:\ \mu|_e \in M^n_h(e) \text{ for all } e \in \mathcal{T}_{h_{kl}}\}$$

$$M^{n,c}_{h_{kl}} = \{\mu:\ \mu|_e \in M^n_h(e) \text{ for all } e \in \mathcal{T}_{h_{kl}},\ \mu \text{ is continuous on } \Gamma_{kl}\}.$$

We denote by $M_{h_{kl}}$ any choice of $M^{n,d}_{h_{kl}}$, $M^{n,c}_{h_{kl}}$, or $M^m_{h_{kl}}$ (on matching interfaces).

Remark 3.1
The usual piecewise constant Lagrange multiplier space for RT_0 leads to only O(1) approximation on the interfaces in the case of non-matching grids. With the above choice for mortar space, optimal convergence and, in some cases, superconvergence is recovered for both pressure and velocity (see References [1, 2] for single phase flow and Reference [27] for two-phase flow).

We employ a variant of the mixed finite element method, the expanded mixed method. It has been developed for accurate and efficient treatment of irregular domains (see References [28, 29] for single block and References [1, 25] for multiblock domains). In the context of multiphase flow this method allows for proper treatment of the degeneracies in the diffusion term (see Remark 3.2).

Following Reference [28], let, for $\alpha = \mathrm{w},\ \mathrm{o},\ \mathrm{g}$,

$$\tilde{\mathbf{U}}_\alpha = -\nabla P_\alpha.$$

Then

$$\mathbf{U}_\alpha = \frac{k_\alpha(S_\alpha)K}{\mu_\alpha}\rho_\alpha(\tilde{\mathbf{U}}_\alpha + \rho_\alpha g \nabla D)$$

Let $0 = t_0 < t_1 < t_2 < \cdots$, let $\Delta t^n = t_n - t_{n-1}$, and let $f^n = f(t_n)$. We first state the backward Euler multiblock expanded mixed finite element approximation of the subdomain equations. Let $1 \leqslant k < l \leqslant n_b$ and $n = 1, 2, 3 \ldots$. Denoting $\lambda_\alpha = K/\mu_\alpha$ for single-phase, $\lambda_\alpha = k_\alpha K/\mu_\alpha$ for two-phase, and $\lambda_\alpha = k_\alpha K/B_\alpha\mu_\alpha$ for black oil, we solve for $\mathbf{U}^n_{h,i}|_{\Omega_k} \in \mathbf{V}_{h_k}$, $\tilde{\mathbf{U}}^n_{h,\alpha}|_{\Omega_k} \in \tilde{\mathbf{V}}_{h_k}$, $P^n_{h,\alpha}|_{\Omega_k} \in W_{h_k}$,

and $N^n_{h,i}|_{\Omega_k} \in W_{h_k}$ satisfying

$$\int_{\Omega_k} \frac{(\phi N_{h,i})^n - (\phi N_{h,i})^{n-1}}{\Delta t^n} w \, \mathrm{d}x + \int_{\Omega_k} \nabla \cdot \mathbf{U}^n_{h,i} w \, \mathrm{d}x = \int_{\Omega_k} q_i \, w \, \mathrm{d}x, \quad w \in W_{h_k} \tag{14}$$

$$\int_{\Omega_k} \tilde{\mathbf{U}}^n_{h,\alpha} \cdot \mathbf{v} \, \mathrm{d}x = \int_{\Omega_k} P^n_{h,\alpha} \nabla \cdot \mathbf{v} \, \mathrm{d}x - \int_{\partial\Omega_k \setminus \partial\Omega} P^{M,n}_{h,\alpha} \mathbf{v} \cdot \nu_k \, \mathrm{d}\sigma, \quad \mathbf{v} \in \mathbf{V}_{h_k} \tag{15}$$

$$\int_{\Omega_k} \mathbf{U}^n_{h,i} \cdot \tilde{\mathbf{v}} \, \mathrm{d}x = \int_{\Omega_k} \lambda^n_\alpha \rho^n_\alpha (\tilde{\mathbf{U}}^n_{h,\alpha} + \rho^n_\alpha g \nabla D) \cdot \tilde{\mathbf{v}} \, \mathrm{d}x, \quad \tilde{\mathbf{v}} \in \tilde{\mathbf{V}}_{h_k} \tag{16}$$

$$\begin{aligned} \int_{\Omega_k} \mathbf{U}^n_{h,G} \cdot \tilde{\mathbf{v}} \, \mathrm{d}x = & \int_{\Omega_k} \lambda^n_{\mathrm{g}} \rho^n_{\mathrm{g}} (\tilde{\mathbf{U}}^n_{h,g} + \rho^n_{\mathrm{g}} g \nabla D) \cdot \tilde{\mathbf{v}} \, \mathrm{d}x \\ & + \int_{\Omega_k} R_{\mathrm{s}} \lambda^n_{\mathrm{o}} \rho^n_{\mathrm{o}} (\tilde{\mathbf{U}}^n_{h,o} + \rho^n_{\mathrm{o}} g \nabla D) \cdot \tilde{\mathbf{v}} \, \mathrm{d}x, \quad \tilde{\mathbf{v}} \in \tilde{\mathbf{V}}_{h_k}. \end{aligned} \tag{17}$$

Equations (14)–(16) hold for $\alpha = \mathrm{w}$ and $i = \mathrm{W}$ on a single-phase block, for $\alpha = \mathrm{w}, \mathrm{o}$ and $i = \mathrm{W}, \mathrm{O}$ on a two-phase block, and for $\alpha = \mathrm{w}, \mathrm{o}, \mathrm{g}$ and $i = \mathrm{W}, \mathrm{O}, \mathrm{G}$ on a black-oil block, except for (16) which does not hold for gas. Equation (17) should be used in this case instead. The phase pressures on the interface are approximated by the mortar finite element variables $P^{M,n}_{h,\alpha}|_{\Gamma_{kl}} \in M_{h_{kl}}$. Finally, the flux continuity is imposed weakly

$$\int_{\Gamma_{kl}} [\mathbf{U}^n_{h,i} \cdot \nu]_{kl} \, \mu \, \mathrm{d}\sigma = 0, \quad \mu \in M_{h_{kl}} \tag{18}$$

where $i = \mathrm{W}$ on Γ^1, $i = \mathrm{W}, \mathrm{O}$ on Γ^2, and $i = \mathrm{W}, \mathrm{O}, \mathrm{G}$ on Γ^3.

Remark 3.2

Introducing the pressure gradients $\tilde{\mathbf{U}}_\alpha$ in the expanded mixed method allows for proper handling of the degenerate (for $S_\alpha = 0$) relative permeability $k_\alpha(S_\alpha)$ in (15)–(16). It also allows, even for a full permeability tensor K, to accurately approximate the mixed method on each subdomain by cell-centred finite differences for N_i and P_α. This is achieved by approximating the vector integrals in (6) and (11) by a trapezoidal quadrature rule and eliminating $\tilde{\mathbf{U}}_{h,\alpha}$ and $\mathbf{U}_{h,i}$ from the system [28, 29]. Relationships (6) and (11) allow for further eliminations and the number of primary variables is reduced to the number of phases. In our case the choices are P_{w} for single-phase, P_{o} and N_{O} for two-phase, and P_{w}, N_{O}, and N_{G} for black-oil.

Remark 3.3

A necessary condition for solvability of the scheme is that, for any $\varphi \in M_{h_{kl}}$,

$$Q_{h,k}\varphi = Q_{h,l}\varphi = 0 \Rightarrow \varphi = 0 \tag{19}$$

where $Q_{h,k}$ is the L^2-projection onto $\mathbf{V}_{h_k} \cdot \nu_k$. This condition requires that the mortar grid is not too fine compared to the subdomain grids and is easily satisfied in practice (see References [1, 2] for details).

4. SOLUTION OF THE ALGEBRAIC SYSTEM

To solve the discrete system (14)–(18) on each time step, we reduce it to an interface problem in the mortar space. This approach is based on a domain decomposition algorithm for single phase flow developed originally for conforming grids [5], and later generalized to non-matching grids coupled with mortars [1]. The core step in this algorithm is solving in parallel a series of subdomain problems with specified Dirichlet boundary conditions.

4.1. Reduction to an interface problem

Let

$$\mathbf{M}_h^1 = \bigoplus_{\Gamma_{kl}\in\Gamma^1} M_{hkl}, \quad \mathbf{M}_h^2 = \bigoplus_{\Gamma_{kl}\in\Gamma^2} M_{hkl}\times M_{hkl}, \quad \mathbf{M}_h^3 = \bigoplus_{\Gamma_{kl}\in\Gamma^3} M_{hkl}\times M_{hkl}\times M_{hkl}$$

be the mortar finite element spaces on Γ^1, Γ^2, and Γ^3, respectively. We define non-linear interface bivariate forms $b^j : \mathbf{M}_h^j \times \mathbf{M}_h^j \to \mathbf{R}$ on Γ^j $(j = 1, 2, 3)$ as follows. For $\psi^j \in \mathbf{M}_h^j$ and $\mu^j \in \mathbf{M}_h^j$ let

$$b^j(\psi^j, \mu^j) = \sum_{\Gamma_{kl}\in\Gamma^j} \int_{\Gamma_{kl}} [\mathbf{U}^j(\psi^j)\cdot v]_{kl}\cdot \mu^j \,\mathrm{d}\sigma$$

where $\mathbf{U}^j(\psi^j)$ are solutions to the series of subdomain problems (14)–(17) with boundary data $P_\alpha^M(\psi^j)$. Here and for the rest of the paper we omit for simplicity the time step and the discretization indexes. To be more precise, on Γ^1 we take

$$\psi^1 = P_{\mathrm{w}}^M, \quad \mathbf{U}^1 = \mathbf{U}_{\mathrm{W}}.$$

On Γ^2 we have the following choices for interface primary variables and corresponding fluxes:

$$\psi^2, \mathbf{U}^2 = \begin{cases} (P_{\mathrm{o}}^M, P_{\mathrm{w}}^M), & (\mathbf{U}_{\mathrm{O}}, \mathbf{U}_{\mathrm{W}}) \\ (P_{\mathrm{o}}^M, N_{\mathrm{O}}^M), & (\mathbf{U}_{\mathrm{O}}, \mathbf{U}_{\mathrm{W}}) \\ (P_{\mathrm{w}}^M, N_{\mathrm{O}}^M), & (\mathbf{U}_{\mathrm{W}}, \mathbf{U}_{\mathrm{O}}). \end{cases}$$

Note that the missing pressure in each of the last two choices can be determined by the capillary pressure relationship (6) and the interface form $b^2(\cdot,\cdot)$ is well defined. The first choice seems to be the natural one. The second one is considered due to its better properties in degenerate conditions (see Section 4.4 below). The third one is the only possible choice on a two-phase – black-oil interface, since black-oil phase equilibrium calculations must be performed on the interface. For the same reason the only choice on Γ^3 is

$$\psi^3 = (P_{\mathrm{w}}^M, N_{\mathrm{O}}^M, N_{\mathrm{G}}^M), \quad \mathbf{U}^3 = (\mathbf{U}_{\mathrm{W}}, \mathbf{U}_{\mathrm{O}}, \mathbf{U}_{\mathrm{G}}).$$

We note that different orders of fluxes could be chosen on Γ^2 or Γ^3, but this would unnecessarily increase the non-linearity of the interface operator.

Let

$$\mathbf{M}_h = \mathbf{M}_h^1 \times \mathbf{M}_h^2 \times \mathbf{M}_h^3$$

denote the mortar space on $\Gamma = \Gamma^1 \cup \Gamma^2 \cup \Gamma^3$. We define $b : \mathbf{M}_h \times \mathbf{M}_h \to \mathbf{R}$ on Γ for $\psi = (\psi^1, \psi^2, \psi^3)$ and $\mu = (\mu^1, \mu^2, \mu^3)$ such that

$$b(\psi, \mu) = b^1(\psi^1, \mu^1) + b^2(\psi^2, \mu^2) + b^3(\psi^3, \mu^3).$$

We now define a non-linear interface operator $B : \mathbf{M}_h \to \mathbf{M}_h$ by

$$\langle B\psi, \mu \rangle = b(\psi, \mu), \quad \forall \mu \in \mathbf{M}_h$$

where $\langle \cdot, \cdot \rangle$ is the L^2-inner product in $\mathbf{M}_h$. It is easy to see that

$$(P_\alpha(\psi), N_i(\psi), \mathbf{U}_i(\psi), P_\alpha^M(\psi))$$

is the solution to (14)–(18), where $\psi \in \mathbf{M}_h$ solves

$$B(\psi) = 0. \tag{20}$$

The operator B is a Dirichlet to Neumann operator

$$B : D \to N$$

where D is the set of primary mortar variables and N is the set of corresponding boundary fluxes.

4.2. *Cost of the interface operator evaluation*

The non-linear iterative solvers for (20) described in the next section require evaluation of the interface operator at each iteration. Here is the algorithm for evaluating $B(\psi)$.

Algorithm 1. `feval`(ψ)

1. Project (orthogonally) mortar data onto the subdomain grids
$$P_\alpha^M(\psi) \xrightarrow{Q_k} \bar{P}_{\alpha,k}.$$
2. Solve in parallel subdomain problems (14)–(17) with boundary conditions $\bar{P}_{\alpha,k}$ to compute $\mathbf{U}_{i,k}$ on each Ω_k.
3. Project boundary fluxes back to the mortar space
$$\mathbf{U}_{i,k} \cdot v_k \xrightarrow{Q_k^T} \mathbf{U}_{i,k}^M.$$
4. Compute flux jump in the mortar space. On each Γ_{kl}
$$[\mathbf{U}_i^M]_{kl} = \mathbf{U}_{i,k}^M + \mathbf{U}_{i,l}^M.$$

The evaluation of B involves solving subdomain problems in parallel and two inexpensive projection steps — from the mortar grid onto the local subdomain grids and from the local grids onto the mortar grid. The subdomain problems are also non-linear and are solved by a preconditioned Newton–Krylov solver [30–32].

4.3. Iterative solution of the interface problem

We discuss two methods for the solution of (20): an inexact Newton-GMRES method and a FAS mortar multigrid with Newton-GMRES smoothing.

4.3.1. Newton-GMRES solver. The inexact Newton step s_k in

$$\psi^{(k+1)} = \psi^{(k)} + s_k$$

is computed by a forward difference GMRES iteration for solving $B'(\psi^{(k)})s_k = -B(\psi^{(k)})$. On each GMRES iteration the action of the Jacobian $B'(\psi)$ on a vector μ is approximated by the forward difference

$$D_\delta B(\psi : \mu) = \frac{B(\psi + \delta\mu) - B(\psi)}{\delta}.$$

The inexact Newton-GMRES algorithm is described in Reference [15]. We present here for completeness the forward difference GMRES iteration for approximating the solution to $B'(\psi)s = -B(\psi)$.

Algorithm 2. `fdgmres`$(s, \psi, B, \delta, \eta, k\max, \rho)$

1. $s = 0,\ r = -B(\psi),\ v_1 = r/\|r\|_2,\ \rho = \|r\|_2,\ \beta = \rho,\ k = 0$
2. While $\rho > \eta$ and $k < k\max$ do
   (a) $k = k + 1$
   (b) $v_{k+1} = D_\delta B(\psi : v_k)$
   (c) for $j = 1, \ldots k$
   $h_{jk} = (v_j, v_{k+1})$
   $v_{k+1} = v_{k+1} - h_{jk} v_j$
   (d) $h_{k+1,k} = \|v_{k+1}\|_2$
   (e) $v_{k+1} = v_{k+1}/\|v_{k+1}\|_2$
   (f) $e_1 = (1, 0, \ldots, 0)^{\mathrm{T}} \in R^{k+1}$
   Find $y_k \in R^k$ that solves $\min_{R^k} \|\beta e_1 - H_k y_k\|_{R^{k+1}}$
   (g) $\rho = \|\beta e_1 - H_k y_k\|_{R^{k+1}}$
3. $s = V_k y_k$.

Remark 4.1
The cost of the most expensive GMRES step

$$v_{k+1} = D_\delta B(\psi : v_k) \tag{21}$$

can be substantially reduced if the latest subdomain solution is used as an initial guess. Since only the boundary data is $O(\delta)$ perturbed, the subdomain solves typically converge in one non-linear iteration.

4.3.2. FAS mortar multigrid V-cycle. Multigrid methods for mortar finite element discretizations of linear elliptic problems have been studied recently [33, 34, 8]. Our approach is based on the one presented in Reference [8]. In its non-linear version it uses the Newton-GMRES

algorithm from the previous section as a smoother. We define a sequence of nested mortar spaces

$$\mathbf{M}_1 \subset \mathbf{M}_2 \subset \cdots \subset \mathbf{M}_J = \mathbf{M}.$$

Each space $\mathbf{M}_j$, $1 \leqslant j \leqslant J$, is associated with a mortar grid $\mathcal{T}_{h_j}^{\Gamma}$ and an interface operator $B_j : \mathbf{M}_j \to \mathbf{M}_j$ as defined in Section 4.1. The intergrid transfer operators are defined as follows.

Coarse to fine $\mathcal{I}_j : \mathbf{M}_{j-1} \to \mathbf{M}_j$,

$$\mathcal{I}_j \mu_{j-1} = \mu_{j-1}, \quad \mu_{j-1} \in \mathbf{M}_{j-1}.$$

Note that $\mathcal{I}_j$ is the identity operator on $\mathbf{M}_{j-1}$.

Fine to coarse $\mathcal{Q}_{j-1} : \mathbf{M}_j \to \mathbf{M}_{j-1}$,

$$\langle \mathcal{Q}_{j-1}\psi_j, \mu_{j-1} \rangle = \langle \psi_j, \mathcal{I}_j \mu_{j-1} \rangle, \quad \psi_j \in M_j, \ \ \mu_{j-1} \in M_{j-1}.$$

Note that $\mathcal{Q}_{j-1}$ is the orthogonal projection onto M_{j-1} and the transpose of $\mathcal{I}_j$.

The FAS multigrid V-cycle is defined as an iterative process for solving $B(\psi) = r$:

$$\psi_{(n+1)} = MG(\psi_{(n)}, r)$$

where $MG = MG_J$ is the multigrid operator defined recursively.

Algorithm 3. $MG_j(g_j, r_j)$ $(1 \leqslant j \leqslant J)$

1. (initialization) $\psi_j^{(0)} = g_j$.
2. (pre-smoothing) $\psi_j^{(1)} = \psi_j^{(0)} + s_m(\psi_j^{(0)})$, where $s_m(\psi_j^{(0)})$ is the m-th GMRES iterate for solving $B_j'(\psi_j^{(0)})s = r_j - B_j(\psi_j^{(0)})$.
3. (coarse grid correction) If $j > 1$ then
   (a) Initialize level $j-1$: $\psi_{j-1}^{(0)} = \mathcal{Q}_{j-1}(\psi_j^{(1)})$
   (b) Project residual: $r_{j-1} = B_{j-1}(\psi_{j-1}^{(0)}) + \mathcal{Q}_{j-1}(r_j - B_j(\psi_j^{(1)}))$
   (c) Correct: $\psi_j^{(2)} = \psi_j^{(1)} + \mathcal{I}_j[MG_{j-1}(\psi_{j-1}^{(0)}, r_{j-1}) - \psi_{j-1}^{(0)}]$
4. (post-smoothing) $\psi_j^{(3)} = \psi_j^{(2)} + s_m(\psi_j^{(2)})$
   $MG_j(g_j, r_j) = \psi_j^{(3)}$.

Note that the smoothing step in Algorithm 3 is equivalent to taking an inexact Newton-GMRES step for solving $B_j(\psi_j) = r_j$.

4.4. Properties of the interface operator

It is well known [35] that the Newton convergence depends on the invertibility of the Jacobian matrix. Let us consider the operator on Γ^2 and denote by (ψ_1, ψ_2) and $(\mathbf{U}_1, \mathbf{U}_2)$ the pairs of primary mortar variables and resulting flux jumps, respectively. The Jacobian matrix has the 2×2 block structure

$$B' = \begin{pmatrix} \frac{\partial \mathbf{U}_1}{\partial \psi_1} & \frac{\partial \mathbf{U}_1}{\partial \psi_2} \\ \frac{\partial \mathbf{U}_2}{\partial \psi_1} & \frac{\partial \mathbf{U}_2}{\partial \psi_2} \end{pmatrix}.$$

Since the flux of a given phase depends more strongly on this phase pressure, we take ψ_1 and $\mathbf{U}_1$ to be the pressure and the flux of same phase. For the three primary mortar choices we then have the interface operators

$$B: \begin{array}{l} (P_{\mathrm{o}}^M, P_{\mathrm{w}}^M) \to (\mathbf{U}_{\mathrm{O}}^M, \mathbf{U}_{\mathrm{W}}^M) \\ (P_{\mathrm{o}}^M, N_{\mathrm{O}}^M) \to (\mathbf{U}_{\mathrm{O}}^M, \mathbf{U}_{\mathrm{W}}^M) \\ (P_{\mathrm{w}}^M, N_{\mathrm{O}}^M) \to (\mathbf{U}_{\mathrm{W}}^M, \mathbf{U}_{\mathrm{O}}^M) \end{array}$$

The first choice leads to the simplest interface operator since it can be viewed as a composite of two single phase Poincare–Steklov maps. Indeed, in this case the Jacobian matrix can be reasonably well approximated by its block-diagonal

$$B'(P_{\mathrm{o}}^M, P_{\mathrm{w}}^M) = \begin{pmatrix} \frac{\partial \mathbf{U}_{\mathrm{O}}^M}{\partial P_{\mathrm{o}}^M} & \frac{\partial \mathbf{U}_{\mathrm{O}}^M}{\partial P_{\mathrm{w}}^M} \\ \frac{\partial \mathbf{U}_{\mathrm{W}}^M}{\partial P_{\mathrm{o}}^M} & \frac{\partial \mathbf{U}_{\mathrm{W}}^M}{\partial P_{\mathrm{w}}^M} \end{pmatrix} \sim \begin{pmatrix} \frac{\partial \mathbf{U}_{\mathrm{O}}^M}{\partial P_{\mathrm{o}}^M} & 0 \\ 0 & \frac{\partial \mathbf{U}_{\mathrm{W}}^M}{\partial P_{\mathrm{w}}^M} \end{pmatrix}.$$

This mapping, however, becomes degenerate when the relative permeability $k_\alpha(S_\alpha)$ of one of the phases is zero on the interface. For example, if $k_{\mathrm{w}} = 0$, then $\mathbf{U}_{\mathrm{W}}^M = 0$ independently of the phase pressures P_α^M and the second row of the Jacobian matrix becomes zero. Note that the second choice $(\psi_1, \psi_2) = (P_{\mathrm{o}}^M, N_{\mathrm{O}}^M)$ leads to a non-degenerate operator in this case, since $\partial \mathbf{U}_{\mathrm{w}}^M / \partial N_{\mathrm{O}}^M$ is non-zero. The map is, however, degenerate if $k_{\mathrm{o}} = 0$. In Section 4.5 we discuss a careful construction of a preconditioner for the Jacobian matrix that handles the degeneracies in each case.

4.5. Interface GMRES preconditioner

A well known drawback of GMRES is that it may converge very slowly if not preconditioned. This may result in either a very expensive or a very inexact Newton step. To remedy this we consider a left preconditioned GMRES which is based on solving

$$M^{-1} B'(\psi) s = -M^{-1} B(\psi)$$

where M is an easily invertible approximation to $B'(\psi)$. The GMRES step (21) now becomes

$$v_{k+1} = M^{-1} D_\delta B(\psi : v_k). \tag{22}$$

Remark 4.2

The preconditioned GMRES is consistent with the underlying physical interpretation of the interface operator B while the unpreconditioned GMRES is not. Recall that $B : \psi \to \mathbf{U}$ is a Dirichlet to Neumann operator. Therefore in (21) the two consecutive Krylov vectors v_k and v_{k+1} have different physical meanings. This inconsistency is corrected by the preconditioner, since

$$M^{-1} : \mathbf{U} \to \psi$$

and

$$M^{-1} D_\delta B(\psi : v_k) : \psi \to \psi$$

Therefore the preconditioned GMRES builds a Krylov basis for the Dirichlet space ψ.

4.5.1. A Neumann–Neumann preconditioner. We write the interface operator B and the approximation to its derivative $D_\delta B$ as sums of local subdomain Dirichlet to Neumann operators

$$B = \sum_k^{n_b} B_k, \qquad D_\delta B = \sum_k^{n_b} D_\delta B_k$$

where B_k ($D_\delta B_k$) involves a subdomain solve on Ω_k with a prescribed Dirichlet boundary data. The Neumann–Neumann preconditioner M^{-1} is defined as a sum of (possibly inexact) local Neumann solves (see Reference [36]):

$$M^{-1} = \sum_k^{n_b} \widehat{D_\delta B_k}^{-1}$$

where $\widehat{D_\delta B_k}^{-1}$ is an approximation to $(D_\delta B_k)^{-1}$. To define $\widehat{D_\delta B_k}^{-1}$ we consider the finite difference approximation of the discrete Darcy's law (15)–(17) and assume that the effect of the boundary pressure is local to the neighbouring cell:

$$\begin{aligned}\hat{B}_{i,k}(P_\alpha^M) &\equiv \hat{\mathbf{U}}_{i,k} \cdot v_k(P_\alpha^M) \\ &= \lambda_{\alpha,k}\rho_{\alpha,k}\left(\frac{P_{\alpha,k} - P_\alpha^M}{h_k/2} + \rho_{\alpha,k} g \nabla D\right), \quad \alpha = \mathrm{w}, \mathrm{o};\ i = \mathrm{W}, \mathrm{O} \end{aligned} \tag{23}$$

$$\begin{aligned}\hat{B}_{\mathrm{G},k}(P_\mathrm{g}^M, P_\mathrm{o}^M) &\equiv \hat{\mathbf{U}}_{\mathrm{G},k} \cdot v_k(P_\mathrm{g}^M, P_\mathrm{o}^M) = \lambda_{\mathrm{g},k}\rho_{\mathrm{g},k}\left(\frac{P_{\mathrm{g},k} - P_\mathrm{g}^M}{h_k/2} + \rho_{\mathrm{g},k} g \nabla D\right) \\ &\quad + R_\mathrm{s}\lambda_{\mathrm{o},k}\rho_{\mathrm{o},k}\left(\frac{P_{\mathrm{o},k} - P_\mathrm{o}^M}{h_k/2} + \rho_{\mathrm{o},k} g \nabla D\right) \end{aligned} \tag{24}$$

where λ_α is defined in (16) and $P_{\alpha,k}$ is the pressure in the cell next to the interface. This leads to approximations

$$\widehat{D_\delta B_{i,k}}(P_\alpha^M : s_{P_\alpha}) = \frac{\hat{B}_{i,k}(P_\alpha^M + \delta s_{P_\alpha}) - \hat{B}_{i,k}(P_\alpha^M)}{\delta} = -2\frac{\lambda_{\alpha,k}\rho_{\alpha,k}}{h_k} s_{P_\alpha} \equiv \beta_{\alpha,k} s_{P_\alpha} \tag{25}$$

and

$$\widehat{D_\delta B_{\mathrm{G},k}}(P_\mathrm{g}^M, P_\mathrm{o}^M : s_{P_\mathrm{o}}, s_{P_\mathrm{g}}) = -2\frac{\lambda_{\mathrm{g},k}\rho_{\mathrm{g},k}}{h_k} s_{P_\mathrm{g}} - 2R_\mathrm{s}\frac{\lambda_{\mathrm{o},k}\rho_{\mathrm{o},k}}{h_k} s_{P_\mathrm{o}} \equiv \beta_{\mathrm{g},k} s_{P_\mathrm{g}} + R_\mathrm{s}\beta_{\mathrm{o},k} s_{P_\mathrm{o}}. \tag{26}$$

4.5.2. A preconditioner for $D_\delta B : P_\mathrm{w}^M \to \mathbf{U}_\mathrm{W}^M$. In this case (25) gives, for a mortar flux v_W^M,

$$M^{-1}(v_\mathrm{W}^M) = \sum_k^{n_b} \frac{1}{\beta_{\mathrm{w},k}} v_\mathrm{W}^M \equiv \frac{1}{\beta_\mathrm{w}} v_\mathrm{W}^M$$

which is just a diagonal scaling.

4.5.3. A preconditioner for $D_\delta B : (P_o^M, P_w^M) \to (\mathbf{U}_O^M, \mathbf{U}_W^M)$. As a first step the Jacobian matrix $B_k'(P_w^M, P_n^M)$ is approximated by its block-diagonal

$$B_k'(P_o^M, P_w^M) = \begin{pmatrix} \frac{\partial \mathbf{U}_{O,k}^M}{\partial P_o^M} & \frac{\partial \mathbf{U}_{O,k}^M}{\partial P_w^M} \\ \frac{\partial \mathbf{U}_{W,k}^M}{\partial P_o^M} & \frac{\partial \mathbf{U}_{W,k}^M}{\partial P_w^M} \end{pmatrix} \sim \begin{pmatrix} \frac{\partial \mathbf{U}_{O,k}^M}{\partial P_o^M} & 0 \\ 0 & \frac{\partial \mathbf{U}_{W,k}^M}{\partial P_w^M} \end{pmatrix}.$$

The preconditioner M^{-1} is now defined from (25) for a given mortar flux (v_O^M, v_W^M)

$$M^{-1} \begin{pmatrix} v_O^M \\ v_W^M \end{pmatrix} = \sum_k^{n_b} \begin{pmatrix} \frac{1}{\beta_{o,k}} & 0 \\ 0 & \frac{1}{\beta_{w,k}} \end{pmatrix} \begin{pmatrix} v_O^M \\ v_W^M \end{pmatrix} \equiv \begin{pmatrix} 1/\beta_o & 0 \\ 0 & 1/\beta_w \end{pmatrix} \begin{pmatrix} v_O^M \\ v_W^M \end{pmatrix}.$$

In the above derivation we assumed that the phase mobilities λ_α are non-zero. In the degenerate cases we need to modify the definition of the preconditioner. Let us consider the case $\lambda_w = 0$ (the case $\lambda_o = 0$ is treated similarly). In this case we set

$$M^{-1} \begin{pmatrix} v_O^M \\ v_W^M \end{pmatrix} = \begin{pmatrix} 1/\beta_o & 0 \\ 1/\beta_o & 1 \end{pmatrix} \begin{pmatrix} v_O^M \\ v_W^M \end{pmatrix} = \begin{pmatrix} v_O^M/\beta_o \\ v_O^M/\beta_o \end{pmatrix}$$

since $v_W^M = 0$, forcing the change in P_o^M and P_w^M to be the same. The capillary pressure relation (6) implies that S_w^M would not change which is consistent with the physical behaviour.

4.5.4. A preconditioner for $D_\delta B : (P_o^M, N_O^M) \to (\mathbf{U}_O^M, \mathbf{U}_W^M)$. Following the derivation in the previous case and using (25) we have

$$\widehat{D_\delta B}_k(P_o^M, N_O^M : s_{P_o}, s_{N_O}) = \begin{pmatrix} \beta_{o,k} s_{P_o} \\ \beta_{w,k} s_{P_w}(s_{P_o}, s_{N_O}) \end{pmatrix}.$$

To express s_{P_w} as a function of (s_{P_o}, s_{N_O}). we must use the capillary pressure (6). Inverting this non-linear function would lead to a non-linear preconditioner so we use instead a linear fit

$$\bar{p}_c(N_O) = aN_O + b$$

where a and b are determined using (6). We now have

$$P_w^M + s_{P_w} = P_o^M + s_{P_o} - \bar{p}_c(N_O^M + s_{N_O})$$

leading to

$$s_{P_w} = s_{P_o} - a s_{N_O}$$

and

$$\widehat{D_\delta B}_k(P_o^M, N_O^M : s_{P_o}, s_{N_O}) = \begin{pmatrix} \beta_{o,k} & 0 \\ \beta_{w,k} & -a\beta_{w,k} \end{pmatrix} \begin{pmatrix} s_{P_o} \\ s_{N_O} \end{pmatrix}$$

We now define M^{-1} for a given mortar flux $(v_{\mathrm{O}}^M, v_{\mathrm{W}}^M)$

$$M^{-1}\begin{pmatrix} v_{\mathrm{O}}^M \\ v_{\mathrm{W}}^M \end{pmatrix} = \sum_k^{n_{\mathrm{b}}} \begin{pmatrix} 1/\beta_{\mathrm{o},k} & 0 \\ 1/(a\beta_{\mathrm{o},k}) & -1/(a\beta_{\mathrm{w},k}) \end{pmatrix} \begin{pmatrix} v_{\mathrm{O}}^M \\ v_{\mathrm{W}}^M \end{pmatrix}$$

$$= \begin{pmatrix} 1/\beta_{\mathrm{o}} & 0 \\ 1/(a\beta_{\mathrm{o}}) & -1/(a\beta_{\mathrm{w}}) \end{pmatrix} \begin{pmatrix} v_{\mathrm{O}}^M \\ v_{\mathrm{W}}^M \end{pmatrix}$$

which is well defined for non-zero mobilities λ_α. If $\lambda_{\mathrm{w}} = 0$ we set

$$M^{-1}\begin{pmatrix} v_{\mathrm{O}}^M \\ v_{\mathrm{W}}^M \end{pmatrix} = \begin{pmatrix} 1/\beta_{\mathrm{o}} & 0 \\ 0 & 1 \end{pmatrix} \begin{pmatrix} v_{\mathrm{O}}^M \\ v_{\mathrm{W}}^M \end{pmatrix} = \begin{pmatrix} v_{\mathrm{O}}^M/\beta_{\mathrm{o}} \\ 0 \end{pmatrix}.$$

If $\lambda_{\mathrm{o}} = 0$ we set

$$M^{-1}\begin{pmatrix} v_{\mathrm{O}}^M \\ v_{\mathrm{W}}^M \end{pmatrix} = \begin{pmatrix} 0 & 1/\beta_{\mathrm{w}} \\ 1 & 0 \end{pmatrix} \begin{pmatrix} v_{\mathrm{O}}^M \\ v_{\mathrm{W}}^M \end{pmatrix} = \begin{pmatrix} v_{\mathrm{W}}^M/\beta_{\mathrm{w}} \\ 0 \end{pmatrix}.$$

Both cases force the correct change in P_{o}^M and no change in N_{O}^M.

4.5.5. A preconditioner for $D_\delta B : (P_{\mathrm{w}}^M, N_{\mathrm{O}}^M) \to (\mathbf{U}_{\mathrm{W}}^M, \mathbf{U}_{\mathrm{O}}^M)$. Similarly to the previous section we have in the non-degenerate case

$$M^{-1}\begin{pmatrix} v_{\mathrm{W}}^M \\ v_{\mathrm{O}}^M \end{pmatrix} = \begin{pmatrix} 1/\beta_{\mathrm{w}} & 0 \\ -1/(a\beta_{\mathrm{w}}) & 1/(a\beta_{\mathrm{o}}) \end{pmatrix} \begin{pmatrix} v_{\mathrm{W}}^M \\ v_{\mathrm{O}}^M \end{pmatrix}.$$

If $\lambda_{\mathrm{o}} = 0$ we set

$$M^{-1}\begin{pmatrix} v_{\mathrm{W}}^M \\ v_{\mathrm{O}}^M \end{pmatrix} = \begin{pmatrix} 1/\beta_{\mathrm{w}} & 0 \\ 0 & 1 \end{pmatrix} \begin{pmatrix} v_{\mathrm{W}}^M \\ v_{\mathrm{O}}^M \end{pmatrix} = \begin{pmatrix} v_{\mathrm{W}}^M/\beta_{\mathrm{w}} \\ 0 \end{pmatrix}.$$

If $\lambda_{\mathrm{w}} = 0$ we set

$$M^{-1}\begin{pmatrix} v_{\mathrm{W}}^M \\ v_{\mathrm{O}}^M \end{pmatrix} = \begin{pmatrix} 0 & 1/\beta_{\mathrm{o}} \\ 1 & 0 \end{pmatrix} \begin{pmatrix} v_{\mathrm{W}}^M \\ v_{\mathrm{O}}^M \end{pmatrix} = \begin{pmatrix} v_{\mathrm{O}}^M/\beta_{\mathrm{o}} \\ 0 \end{pmatrix}.$$

Again the correct change in P_{w}^M and no change in N_{O}^M is forced.

Remark 4.3

In all of the cases considered above the computational cost for the preconditioner is negligible. It involves either diagonal scaling or trivial local multiplication by a 2×2 matrix.

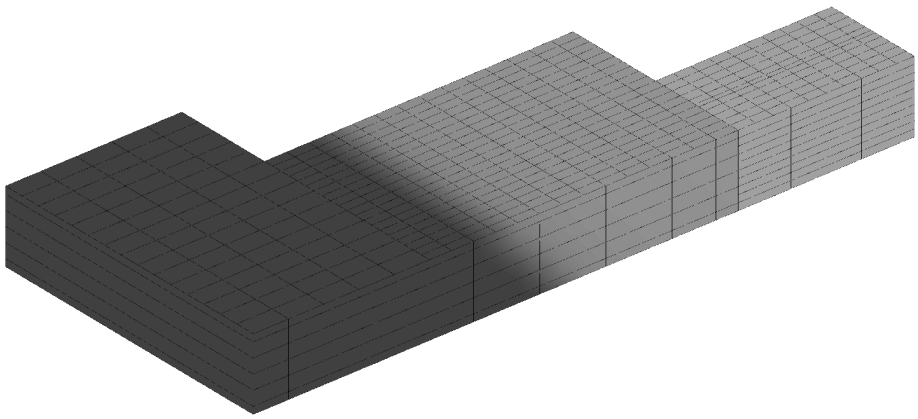

Figure 1. Numerical grids and initial fluid distribution.

4.5.6. A preconditioner for $D_\delta B : (P_{\mathrm{w}}^M, N_{\mathrm{O}}^M, N_{\mathrm{O}}^G) \to (\mathbf{U}_{\mathrm{W}}^M, \mathbf{U}_{\mathrm{O}}^M, \mathbf{U}_{\mathrm{G}}^M)$. Following the derivation in the previous cases, and using (25) and (26) we arrive at

$$\widehat{D_\delta B}_k(P_{\mathrm{w}}^M, N_{\mathrm{O}}^M, N_{\mathrm{G}}^M : s_{P_{\mathrm{w}}}, s_{N_{\mathrm{O}}}, s_{N_{\mathrm{G}}}) = \begin{pmatrix} \beta_{\mathrm{w},k} s_{P_{\mathrm{w}}} \\ \beta_{\mathrm{o},k} s_{P_{\mathrm{o}}} \\ \beta_{\mathrm{g},k} s_{P_{\mathrm{g}}} + R_{\mathrm{s}} \beta_{\mathrm{o},k} s_{P_{\mathrm{o}}} \end{pmatrix}.$$

We express $s_{P_{\mathrm{o}}} = s_{P_{\mathrm{o}}}(s_{P_{\mathrm{w}}}, s_{N_{\mathrm{O}}}, s_{N_{\mathrm{G}}})$ and $s_{P_{\mathrm{g}}} = s_{P_{\mathrm{g}}}(s_{P_{\mathrm{w}}}, s_{N_{\mathrm{O}}}, s_{N_{\mathrm{G}}})$ using a linearized version of (11). We do not give details.

5. COMPUTATIONAL RESULTS

In this section we present multiphysics simulations illustrating the efficiency of the non-linear interface solvers described in the previous section. We consider a three-block dipping reservoir. The initial hydrostatic fluid distribution is given in Figure 1. Due to gravity only water (the darker shade) is present below the water–oil contact. Gas phase is only present at the top above a specified gas–oil contact. A production well is placed near the top and several water-injection wells are placed near the bottom to maintain pressure (see Figure 2). The simulation is performed using single-phase (water) model in the bottom block, a two-phase (oil and water) model in the middle block and a black-oil (oil, water, and gas) model in the top block. The interface primary variables are P_{w}^M on the first interface and $(P_{\mathrm{w}}^M, N_{\mathrm{O}}^M)$ on the second interface. The reader is referred to Reference [3] for a more detailed physical description of the problem.

In all examples the non-linear interface residuals are measured in the l_2 vector norm scaled by $1/\sqrt{N}$, where N is the number of interface variables. The scaling guarantees that the norm of a constant interface function is independent of the mortar grid. The non-linear interface iteration is terminated when the residual norm becomes smaller than 10^{-4}.

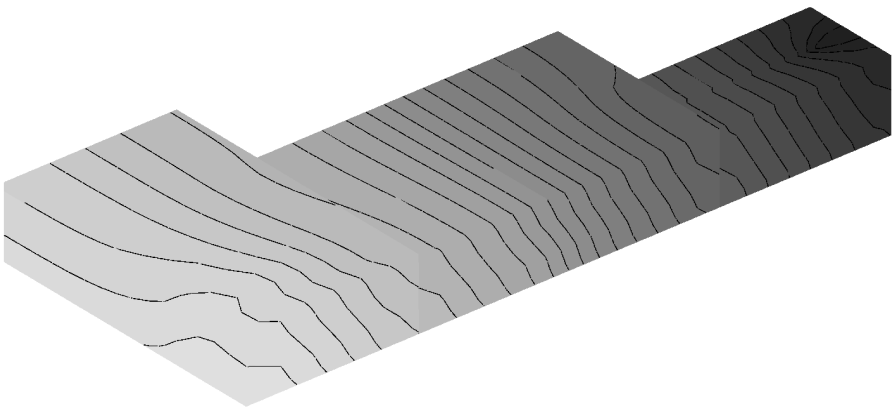

Figure 2. Water pressure contours.

Table I. FAS multigrid performance on a fixed grid.

mg levels	Smoothings	V-cycles	Avg. resid. reduction
2	1	6	0.141
3	1	5	0.092
4	1	5	0.093
2	3	3	0.0064
3	3	3	0.006
4	3	3	0.006

We first study the performance of the interface multigrid. The numerical grids are $5 \times 15 \times 6$ in the bottom block, $14 \times 20 \times 6$ in the middle block, and $10 \times 11 \times 10$ in the top block. Discontinuous piecewise linear mortars on 4×10 and 4×5 grids are used to couple the subdomains. In Table I we report the number of V-cycles and the average residual reduction on a typical time step for various choices of multigrid levels and number of smoothings. We note that for a fixed number of smoothings both the number of V-cycles and the residual reduction are very weakly dependent on the number of multigrid levels. To assess the scalability of the algorithm we also ran the simulation on three additional grids — a coarsening and two levels of refinement of the above grid by a factor of two in each direction (thus increasing the number of degrees of freedom by a factor of eight on each level). The results for three smoothings are given in Table II. The mild dependence of the number of V-cycles and the residual reduction on the size of the problem indicates very good scalability.

In the next study we run the above simulation using the Newton-GMRES interface solver. In particular we are interested in the effect of the GMRES preconditioner on the linear and non-linear convergence. As can be seen in Figure 3 the GMRES preconditioner improves significantly the linear convergence. As a result the desired relative linear tolerance 0.01 is achieved within the prescribed number of GMRES iterations (10 in this case), which is not the case for the unpreconditioned version. We recall that the cost for applying the preconditioner

Table II. FAS multigrid performance on a sequence of refined grids.

Refinement level	Subdomain DOF	Mortar DOF	mg levels	V-cycles	Avg. resid. reduction
1	936	88	2	2	0.005
2	7110	320	3	3	0.006
3	56880	1280	4	4	0.018
4	455040	5120	5	4	0.031

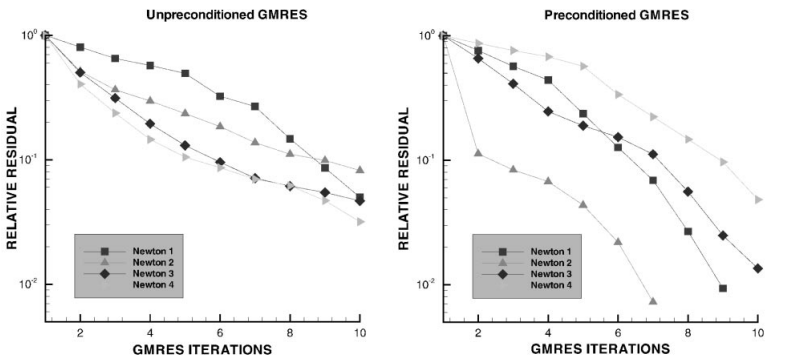

Figure 3. Effect of preconditioner on interface GMRES convergence.

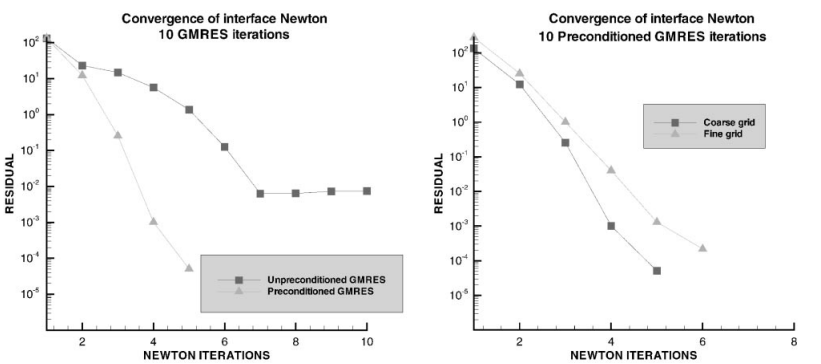

Figure 4. Effect of preconditioner on interface Newton convergence.

is negligible, since it involves either a diagonal scaling or a block-diagonal scaling with 2×2 blocks. The more accurate Newton steps taken with the preconditioned GMRES lead to a much faster (superlinear) interface Newton convergence (see the left plot in Figure 4). We note that the linear solver cost per Newton iteration in both runs is the same, so the overall computational cost is directly proportional to the number of Newton iterations. This is due to the fact that the linear tolerance is set low enough so that the imposed limit of 10 GMRES iterations is always reached.

Finally, we study the scalability of the preconditioned Newton-GMRES solver by running the simulation on a grid refined by two in each direction. The right plot in Figure 4 shows only a slight dependence of the Newton convergence on the size of the problem. Here, as in the left plot, the number of linear iterations per Newton step in both runs equals 10.

6. CONCLUSIONS

We present two methods for solving the non-linear interface algebraic system that arises in the discretization of multiblock multiphysics problems: an inexact Newton-GMRES method and a FAS multigrid V-cycle with Newton-GMRES smoothing. As indicated by the numerical experiments, both algorithms exhibit a very mild dependence of the number of non-linear iterations on the problem size and, in the multigrid case, on the number of grid levels. The overall efficiency strongly depends on the behaviour of the GMRES solver. A Neumann–Neumann preconditioner is constructed that accelerates substantially the GMRES convergence.

ACKNOWLEDGEMENTS

The computational results in this paper were obtained by using the reservoir simulator IPARS developed at the University of Texas at Austin Center for Subsurface Modeling in collaboration with the author. Special thanks are extended to Qin Lu, Manish Parashar, Malgo Peszynska, and Mary Wheeler for their contribution to the development of the multiblock component of the simulator.

REFERENCES

1. Yotov I. Mixed finite element methods for flow in porous media. *PhD Thesis*, Rice University, Houston, Texas, 1996. TR96-09, Dept. Comp. Appl. Math., Rice University and *TICAM Report* 96-23, University of Texas at Austin.
2. Arbogast T, Cowsar LC, Wheeler MF, Yotov I. Mixed finite element methods on non-matching multiblock grids. *SIAM Journal of Numerical Analysis* 2000; **37**:1295–1315.
3. Peszynska M, Lu Q, Wheeler MF. Multiphysics coupling of codes. In *Computational Methods in Water Resources XIII*, Bentley LR *et al.* (eds), Balkema, 2000; 175–182.
4. Peszynska M. Advanced techniques and algorithms for reservoir simulation III. Multiphysics coupling for two phase flow in degenerate conditions. In *Proceedings of IMA Workshop on Reactive Flow and Transport Phenomena*, 2000. To appear.
5. Glowinski R, Wheeler MF. Domain decomposition and mixed finite element methods for elliptic problems. In *First International Symposium on Domain Decomposition Methods for Partial Differential Equations*, Glowinski R, Golub GH, Meurant GA, Periaux J, (eds). SIAM: Philadelphia, 1988, 144–172.
6. Cowsar LC, Wheeler MF. Parallel domain decomposition method for mixed finite elements for elliptic partial differential equations. In *Fourth International Symposium on Domain Decomposition Methods for Partial Differential Equations*, Glowinski R, Kuznetsov Y, Meurant G, Periaux J, Widlund O. (eds). SIAM: Philadelphia, 1991.
7. Cowsar LC, Mandel J, Wheeler MF. Balancing domain decomposition for mixed finite elements. *Mathematical Computing* 1995; **64**:989–1015.
8. Wheeler MF, Yotov I. Multigrid on the interface for mortar mixed finite element methods for elliptic problems. *Computational Methods in Applied Mechanics and Engineering* 2000; **184**:287–302.
9. Wheeler MF, Yotov I. Physical and computational domain decompositions for modeling subsurface flows. In *Tenth International Conference on Domain Decomposition Methods*, Jan Mandel *et al.*, (ed.), *Contemporary Mathematics*, *vol 218*, American Mathematical Society: Providence, RI 1998; 217–228.
10. Kuznetsov YA, Wheeler MF. Optimal order substructuring preconditioners for mixed finite element methods on non-matching grids. *East-West Journal of Numerical Mathematics* 1995; **3**(2):127–143.
11. Achdou Y, Kuznetsov YA, Pironneau O. Substructuring preconditioners for the Q_1 mortar element method. *Numerical Mathematics*, 1995; **71**:419–450.

12. Yves Achdou, Yvon Maday, Olof B. Widlund. Iterative substructuring preconditioners for mortar element methods in two dimensions. *SIAM Journal of Numerical Analysis* 1999; **36**(2):551–580.
13. Cai XC, Dryja M. Domain decomposition methods for monotone non-linear elliptic problems. In *Contemporary Mathematics*, David Keyes et al. (eds), vol 180. American Mathematical Society: Providence, RI 1994; 21–27.
14. Tai X-C, Espedal M. Rate of convergence of some space decomposition methods for linear and non-linear problems. *SIAM Journal of Numerical Analysis* 1998; **35**(4):1558–1570.
15. Kelley CT. *Iterative Methods for Linear and Nonlinear Equations*. SIAM: Philadelphia, 1995.
16. Wolfgang Hackbusch. *Multigrid Methods and Applications*. Springer-Verlag: Berlin, 1985.
17. Lake LW. *Fundamentals of Enhanced Oil Recovery*. Prentice-Hall: NJ, 1989.
18. Peaceman DW. *Fundamentals of Numerical Reservoir Simulation*. Elsevier: Amsterdam, 1977.
19. LU Q, Peszynska M, Wheeler MF, Yotov I. Multiphysics and multinumerics couplings for multiphase flow in porous media. In preparation.
20. Raviart RA, Thomas JM. A mixed finite element method for 2nd order elliptic problems. In *Mathematical Aspects of the Finite Element Method*, *Lecture Notes in Mathematics*, vol. 606. Springer-Verlag: New York, 1977; 292–315.
21. Bernardi C, Maday Y, Patera AT. A new nonconforming approach to domain decomposition: the mortar element method. In *Nonlinear Partial Differential Equations and their Applications*, Brezis H, Lions JL. (eds). Longman Scientific & Technical: UK, 1994.
22. Ben Belgacem F. The mortar finite element method with Lagrange multipliers. *Numerical Mathematics* 1999; **84**(2):173–197.
23. Barbara I. Wohlmuth. A mortar finite element method using dual spaces for the Lagrange multiplier. *SIAM Journal of Numerical Analysis* 2000; **38**(3):989–1012.
24. Ewing R, Lazarov R, Lin T, Lin Y. Mortar finite volume element approximations of second order elliptic problems. *East-West Journal of Numerical Mathematics* 2000; **8**(2):93–110.
25. Yotov I. Mortar mixed finite element methods on irregular multiblock domains. In *Iterative Methods in Scientific Computation*, Wang J, Allen MB, Chen B, Mathew T (eds). *IMACS Series Computation and Applied Mathematics*, *vol. 4,* IMACS, 1998; 239–244.
26. Faker Ben Belgacem. The mixed mortar finite element method for the incompressible Stokes problem: convergence analysis. *SIAM Journal of Numerical Analysis* 2000; **37**(4):1085–1100.
27. Yotov I. A mixed finite element discretization on non-matching multiblock grids for a degenerate parabolic equation arising in porous media flow. *East-West Journal of Numerical Mathematics* 1997; **5**(3):211–230.
28. Arbogast T, Wheeler MF, Yotov I. Mixed finite elements for elliptic problems with tensor coefficients as cell-centered finite differences. *SIAM Journal of Numerical Analysis* 1997; **34**(2):828–852.
29. Arbogast T, Dawson CN, Keenan PT, Wheeler MF, Yotov I. Enhanced cell-centered finite differences for elliptic equations on general geometry. *SIAM Journal on Scientific Computing* 1998; **19**(2):404–425.
30. Dawson CN, Klie H, Wheeler MF, Woodward C. A parallel, implicit, cell-centered method for two-phase flow with a preconditioned Newton–Krylov solver. *Computational Geoscience* 1997; **1**:215–249.
31. Edwards HC. A parallel multilevel-preconditioned GMRES solver for multiphase flow models in the implicit parallel accurate reservoir simulator. *Technical Report* 98-04, TICAM, University of Texas at Austin, 1998.
32. Lacroix S, Vassilevski Y, Wheeler M. Iterative solvers of the Implicit Parallel Accurate Reservoir Simulator (IPARS), I: Single processor case. *Technical Report* 00-28, TICAM, University of Texas at Austin, 2000.
33. Dietrich Braess, Wolfgang Dahmen, Christian Wieners. A multigrid algorithm for the mortar finite element method. *SIAM Journal of Numerical Analysis* 1999; **37**(1):48–69.
34. Jayadeep Gopalakrishnan and Joseph E. Pasciak. Multigrid for the mortar finite element method. *SIAM Journal of Numerical Analysis* 2000; **37**(3):1029–1052.
35. Dennis JE Jr, Schnabel RB. *Numerical Methods for Unconstrained Optimization and Nonlinear Equations*. SIAM: Philadelphia, 1996.
36. De Roeck YH, Le Tallec P. Analysis and test of a local domain decomposition preconditioner. In *Fourth International Symposium on Domain Decomposition Methods for Partial Differential Equations*, Glowinski R, Kuznetsov Y, Meurant G, Periaux J, Widlund O (eds). SIAM: Philadelphia, 1991.

